Received xx xx xxxx; | Revised xx xx xxxx; | Accepted xx xx xxxx

DOI: xxx/xxxx

WILEY ETRI Journal

ORIGINAL ARTICLE

Joint Resource Optimization for NOMA Enhanced SVC Multicast in UAV-Assisted Radio Access Networks

Ziyuan Tong[1] | Hang Shen[1] | Ning Shi[2] | Tianjing Wang[1] | Guangwei Bai[1]

[1]College of Computer Science and Technology, Nanjing Tech University, Nanjing, China
[2]Nanjing Trusted Blockchain and Algorithm Economics Institute, Nanjing, China

Correspondence
Hang Shen, College of Computer Science and Technology, Nanjing Tech University, Nanjing, China.
Email: hshen@njtech.edu.cn

Funding Information
This research was supported by the National Natural Science Foundation of China under Grants 61502230 and 61501224, the National Project Funding for Key R&D Programs under Grant 2018YFC0808500, the Natural Science Foundation of Jiangsu Province under Grant BK20201357, and the Six Talent Peaks Project in Jiangsu Province under Grant RJFW-020.

Abstract

This paper investigates a joint resource optimization scheme for non-orthogonal multiple access (NOMA) enhanced scalable video coding (SVC) multicast in unmanned aerial vehicle (UAV)-assisted radio access networks (RANs). This scheme allows a ground base station and UAVs to simultaneously multicast the successive video layers in SVC with the successive interference cancellation in NOMA. A video quality maximization problem is formulated as a mixed-integer nonlinear programming problem to determine UAV deployment and association, the RAN spectrum allocation for multicast groups, and UAV transmit power. The optimization problem is decoupled into the UAV deployment-association subproblem, spectrum partition subproblem, and UAV transmit power control subproblem. A heuristic strategy is designed to determine UAV deployment and association patterns. An upgraded knapsack algorithm is developed to solve spectrum partition, followed by fast UAV power fine-tuning to boost performance further. Simulation results verify that the proposed scheme improves the average peak signal-to-noise ratio, aggregate video reception rate, and spectrum utilization compared with various baselines.

KEYWORDS:
Non-orthogonal multiple access (NOMA), unmanned aerial vehicle (UAV), scalable video coding (SVC), spectrum partition, transmit power adjustment

†

1 | INTRODUCTION

High-definition video services have become the main driver for the rapidly deployed fifth generation (5G) radio access networks (RANs) [1]. The surge in video traffic results in a shortage of network resources. Video multicast uses the broadcast characteristics of wireless media to improve transmission efficiency. By using the same wireless spectrum resources, multicast can send data from one data source to multiple target end devices (EDs). However, video multicast needs to ensure the reception rate of each ED in a multicast group, where the ED with the worst channel quality incurs a bottleneck of the multicast rate to fulfill the video quality requirement.

Wireless video multicast using scalable video coding (SVC) can alleviate the bottleneck effect brought by EDs experiencing poor channel conditions [2, 3]. SVC separates a video stream into one basic video layer (BL) and multiple enhancement video layers (ELs). EDs can decode different video layers depending on the channel conditions and decoding capabilities. Because of the robust error resistance, the absence of ELs cannot affect the BL's decoding and playback. Even if the EL is lost, the ED can decode the BL to watch the full but lower definition video. In conventional SVC multicast confined to orthogonal multiple access (OMA), each video layer is transmitted over different orthogonal channels with reduced spectrum utilization efficiency. Multiplexing power domain non-orthogonal multiple access (NOMA) can serve

This is an Open Access article distributed under the term of Korea Open Government License (KOGL) Type 4: Source Indication + Commercial Use Prohibition + Change Prohibition (http://www.kogl.or.kr/info/licenseTypeEn.do).

xxxx-xxxx/$ © xxxx ETRI

multiple EDs on the same channel [4]. A transmitter can allocate different powers to each video layer, whose signal power arriving at receivers is different. Receivers demodulate signals via successive interference cancellations (SIC) [5]. In this case, the video quality and resource efficiency achieved by NOMA outperform that by OMA, especially under diverse channel conditions [6].

Unmanned aerial vehicle (UAV)-assisted RAN architecture has excellent potential to enhance SVC video multicast quality and flexibility. First, inherent from terrestrial BSs, video multicast may suffer from low resource utilization and low video quality for EDs at BS's coverage edge. For instance, in some major sports events, concerts, etc., off-site audiences and users with limited viewing angles usually watch live online. BSs in these areas inevitably become overloaded. In this case, UAVs, as air support, can be temporarily deployed with great potential to improve video services. Second, more likely to establish line-of-sight (LoS) communication links, UAVs help to reduce resource consumption in video transmission [7]. Third, UAVs can adjust positions to enhance video reception quality in hotspot areas [8] and improve resource utilization by adjusting transmit power.

The above considerations motivate the development of a UAV-Assisted SVC multicast scheme for NOMA-enabled cellular networks. However, supporting SVC video multicast in NOMA-enhanced networks faces significant challenges in determining UAV deployment and transmit power, the association patterns between UAVs and multicast groups, and resource allocation among multicast groups. First, the optimal multicast group association largely depends on UAV placement and resource allocation. Second, The UAV's transmit power significantly influences the sequential superposition of video layers and resource division among different multicast groups [9]. Third, due to the unique channel model [10], each UAV has an effective coverage area determined by its flying height. Even given UAV locations, the resource allocation must consider its effective coverage.

1.1 | Related Works

Most existing works study resource management for SVC multicast in terrestrial networks, in which the optimization of power allocation is one of the research hotspots. Zhu *et al*. explore multi-group resource allocation and intra-group power allocation [2]. Wu *et al*. investigate the NOMA downlink relay transmission, in which the vertical decomposition is adapted, and a layered power allocation algorithm is proposed to maximize throughput [11]. Liu *et al*. propose cooperative NOMA broadcasting/multicasting for vehicle-to-everything to improve service and fairness. The formulated problem is transformed into a sequence of convex feasibility problems and solved by a bisection-based power allocation algorithm [12]. Ahn *et al*. investigate a cross-layer collaboration between SVC and layered-division multiplexing to enhance the reliability gain of broadcast/broadband cooperation [13].

Another research line focuses on user grouping. Zhou *et al*. design cell range expansion and almost blank subframe schemes, addressing the joint optimization of resource allocation and user association for SVC multicast [14]. Araniti *et al*. study the simultaneous transmission of the same content within multiple cells and design a dynamic area formation algorithm to increase the aggregate data rate [15]. Jiang *et al*. propose a novel user grouping strategy in a quality-driven scalable video transmission framework with cross-layer support for multi-user NOMA [16]. By analyzing the reliability and quality gains achieved by a broadcast-unicast convergent platform, Ahn *et al*. propose an optimal broadcast content selection strategy to maximize transmission rates [17].

UAV-assisted resource provisioning has attracted the attention of academia, in which relatively little literature considers the integration with NOMA technology. By optimizing user scheduling and UAV trajectory, Pang *et al*. present a UAV-assisted NOMA network to maximize the sum rate of UAV-served EDs [18]. A mmWave-enabled NOMA-UAV network is presented in [19] to maximize the energy efficiency via optimizing the UAV placement, hybrid precoding, and power allocation. Nguyen *et al*. study the iterative optimization of trajectory control and subchannels assignment for UAV-enabled wireless networks, aiming to maximize the minimum rate of EDs [20]. A joint UAV height optimization, channel allocation, and power allocation scheme is presented to maximize the total rate of cell edge EDs in UAV coverage [21]. Amin *et al*. study UAV-assisted backscatter networks where a UAV acts both as a mobile power transmitter and an information collector. The trade-off among UAV altitude, number of backscatter devices, and backscatter coefficients are identified to maximize the number of decoded bits while minimizing UAV flight duration [22]. A UAV-aided NOMA scheme is explored in [23] to achieve simultaneous wireless information and power transfer while guaranteeing secure transmission for passive ground receivers.

Whether UAV can boost NOMA-enabled SVC multicast remains open to debate, and investigating adaptive resource management and transmit power adjustment is necessary. This paper intends to explore the joint optimization for NOMA enhanced SVC multicast in UAV-assisted RANs and identify the key factors that influence video quality.

1.2 | Contribution and Organization

By considering BS-UAV cooperation, we study a resource management problem for SVC multicast in NOMA-enhanced RANs, aiming to maximize the overall video quality at EDs in multicast groups. The main contributions are as follows:

1. A NOMA-enabled SVC video multicast scheme is proposed, where a BS and UAVs transmit different video layer signals in the power domain on the same channel. The joint optimization of UAV deployment, association pattern, spectrum division, and UAV transmit power adjustment is formulated as a mixed-integer nonlinear programming (MINLP) problem, considering video traffic statistics and environmental factors.

2. The proposed optimization problem is decoupled into the UAV deployment-association (UDA), spectrum partition (SP), and UAV transmit power adjustment (TPA) subproblems. A k-means based heuristic method is adopted to determine UAV deployment and association patterns for the UDA subproblem. An upgraded multiple-choice knapsack is then designed for the SP subproblem to find the number of subchannels for each multicast group, along with a fast power fine-tuning for the TPA subproblem to boost performance further.

3. Simulations demonstrate that the proposed scheme outperforms various baseline methods, significantly reducing complexity with little sacrifice in performance. In terms of average peak signal-to-noise ratio (PSNR), our method is at most 0.7% lower than the optimal solution and hits it directly in most cases.

The rest of the paper is organized as follows. In Section 2, we introduce the network model. Then, the joint optimization and solution are proposed in Section 3 and Section 4, respectively. In Section 5, extensive simulation results are provided to evaluate the performance of our proposed protocol and algorithm. Finally, we conclude our paper in Section 6. The main symbols are listed in Table 1.

TABLE 1 IMPORTANT SYMBOLS

Symbols	Definition
$a_{j,n}$	Association indicator for group n to UAV j
b_n	Number of subchannels allocated to the nth group
B	Total number of subchannels
$e_{j,s}$	Indicator for transmit power s selected by UAV j
$g_{m,i}$	Channel gain from the BS to ED i
$g_{j,i}$	Channel gain from UAV j to ED i
$h_{m,i}$	Horizontal distance between the BS and ED i
$h_{i,j}$	Horizontal distance between ED i and UAV j
$\mathcal{I}_n/I_n$	Set/Number of EDs in multicast group n
$\mathcal{I}_{j,n}/I_{j,n}$	Set/Number of EDs in $\mathcal{I}_n$ covered by UAV j
$\mathcal{J}/J$	Set/Number of UAVs' ID
$\mathcal{N}/N$	Set/Number of multicast groups
$p_{j,s}$	Transmit power s selected by UAV j
p_m	Transmit power of the BS
$\mathrm{PSNR}_{1,n}$	PSNR of the BL received by group n
$\mathrm{PSNR}_{2,n}$	PSNR of the EL and the EL received by group n
R_j	Effective coverage radius of UAV j
$\mathcal{S}_j/S_j$	Set/Number of transmit power indexes for UAV j
$u_{1,n,i}/u_{2,n,i}$	BL/EL reception indicator for ED $i \in \mathcal{I}_n$
v_j	UAV deployment position (x_j, y_j, z_j)
w	Bandwidth of each subchannel
$z^{(\min)}/z^{(\max)}$	Lower/Upper bound of UAV flying height
$\lambda_{l,n}$	Bit rate of the lth video layer requested by group n
$\eta_{\mathrm{LoS}}/\eta_{\mathrm{NLoS}}$	Additional path-loss of the U2E link for LoS/NLoS
ξ	LoS probability theshold
ψ	Free space path-loss threshold

2 | SYSTEM MODEL

Consider a UAV-assisted RAN, where multiple UAVs are placed in the communication coverage of a BS, as shown in Fig. 1. It is assumed that UAVs have high capacity fronthaul links through free space optics or millimeter-wave to communicate with the BS to obtain video content [24]. When necessary, UAVs can harvest power from the BS through wireless power transfer [25]. All EDs are randomly distributed within the BS coverage. EDs requesting the same video stream belong to one multicast group.

2.1 | Layered Video Streams

SVC separates video streams into multiple video layers with different quality-level resolutions, consisting of a BL and multiple ELs. In the system, the BS sends the BL to all the EDs, while UAVs send one EL to the EDs located at hot spots. The BL (EL) is referred to as the first (second) video layer. Denote $\lambda_{l,n}$ as the bit rate of the lth video layer requested by multicast group n, which represents the minimum rate for normal video decoding. The video reception should reach the minimum rate at which the video can be played. Multiple video layers can be reconstructed into a complete video. The EL can be decoded if and only if the BL is completely received.

2.2 | UAV Coverage Model

There exist two types of communication links (i.e., BS-to-ED link (B2E) and UAV-to-ED (U2E) link) in video delivery. Different from the B2E channel, the U2E channel quality is influenced by factors such as UAV flight altitude, elevation angle and probabilities of LoS or non-line-of-sight (NLoS) communications. The location coordinates of ED i is denoted as $(x_i, y_i, 0)$. Let $v_j = (x_j, y_j, z_j)$ represent the deployment

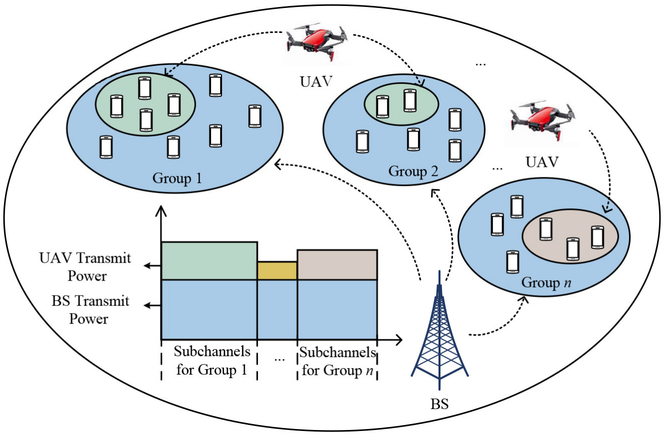

FIGURE 1 UAV-assisted SVC video multicast for multiple groups.

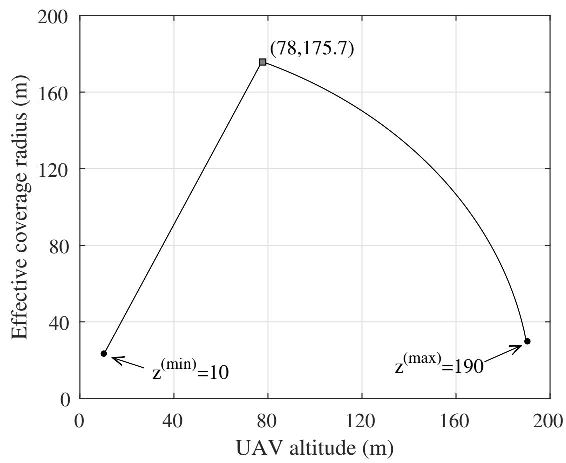

FIGURE 2 Effective UAV coverage.

position of UAV j. The LoS probability between UAV j and ED i is defined as [26]

$$P_{\mathrm{LoS}}(h_{i,j}, z_j) = \frac{1}{1 + o_1 \exp\left(-o_2\left(\arctan(\frac{z_j}{h_{i,j}}) - o_1\right)\right)} \quad (1)$$

where $h_{i,j} = \sqrt{(x_i - x_j)^2 + (y_i - y_j)^2}$ represents the horizontal distance between ED i and UAV j. o_1 and o_2 are constant determined by environmental factors. The average path-loss is given by [26]

$$\phi(h_{i,j}, z_j) = 20\log\left(\frac{4\pi c_1\sqrt{h_{i,j}^2 + z_j^2}}{c_2}\right) + P_{\mathrm{LoS}}\left(h_{i,j}, z_j\right)\eta_{\mathrm{LoS}} + \left(1 - P_{\mathrm{LoS}}(h_{i,j}, z_j)\right)\eta_{\mathrm{NLoS}} \quad (2)$$

where c_1 is the carrier frequency and c_2 is the speed of light. η_{LoS} and η_{NLoS} represent the additional path-loss of the U2E link for LoS reception and NLoS. The channel gain from UAV j to ED i is calculated as $g_{j,i} = 10^{-\frac{\phi(h_{i,j}, z_j)}{10}}$. The effective coverage radius of UAV j depends mainly on LoS probability and free space path-loss, determined as [7, 27]

$$R_j = \min\{\frac{z_j}{\tan\left(o_1 - \frac{1}{o_2}\ln\frac{1-\xi}{o_1\xi}\right)}, \sqrt{\left(\frac{c_2 10^{\frac{\psi}{20}}}{4\pi c_1}\right)^2 - z_j^2}\} \quad (3)$$

where ξ represents the LoS probability for each UAV and ψ represents the threshold of free space path-loss. Fig. 2 shows that the impact of z_j on R_j in this scenario with ξ and ψ of 89dB and 0.5, and o_1 and o_2 of 9.61 and 0.16. UAV flying height ranges from the lower bound of $z^{(\min)}$ =10m to the upper bound of $z^{(\max)}$ =190m. Note that there is no simple linear relationship between z_j and R_j. R_j increases monotonically at first and then decreases with the rise of z_j. When a UAV is flying at the height of 78m, the effective coverage radius reaches its maximum of 175.7m.

2.3 | UAV-Assisted NOMA Video Multicast

Assume that B orthogonal subchannels can be allocated to N multicast groups, and the bandwidth of each subchannel is w. The number of subchannels allocated to multicast group n is denoted as b_n. Each multicast group is allocated different orthogonal subchannels and associated with at most one UAV, as shown in Fig. 1. If transmit power s (denoted by $p_{j,s}$) is chosen by UAV j, indication variable $e_{j,s}$ is set to 1; otherwise, set to 0. If multicast group n is associated with UAV j, indication variable $a_{j,n}$ is set to 1; otherwise, set to 0. The transmit power of the BS is denoted as p_m. Take Fig. 3 as an example to explain the cooperation between the BS and UAV j for multicast group n. The BS propagates the BL through the first NOMA layer using transmit power p_m, while UAV j transmits the EL via the second NOMA layer using transmit power $p_{j,s}$. These signals can be superimposed and coded in the power domain. Let $\mathcal{S}_j$ denote the index set of optional transmit power for UAV j, with S_j being its set cardinality. Denote $\mathcal{J}$ as the ID set of available UAVs. The transmit power for subchannels allocated to multicast group n is

$$p_m + \sum_{j\in\mathcal{J}}\sum_{s\in\mathcal{S}_j} a_{j,n}e_{j,s}p_{j,s}.$$

The receivers at EDs can conduct the SIC decoding.

Let (x_m, y_m, z_m) denote the location coordinates of the BS. The set of EDs in multicast group n and its set cardinality are denoted as $\mathcal{I}_n$ and I_n. When multicast group n receives signals of the BL, the B2E channel gain from the BS to ED $i \in \mathcal{I}_n$ is calculated as $g_{m,i} = 10^{-\frac{\left(\sqrt{h_{m,i}^2 + z_m^2}\right)^{\gamma}}{10}}$, where $h_{m,i} = \sqrt{(x_i - x_m)^2 + (y_i - y_m)^2}$ represents the horizontal distance between the BS and ED i and γ is the path-loss exponent. Since the BL's signals from the BS is interfered with by that of the EL from UAV j with $p_{j,s}$, the achievable rate of decoding the BL's signals at ED $i \in \mathcal{I}_n$ is expressed as a function of $\mathcal{A}_n = \bigcup_{j\in\mathcal{J}} a_{j,n}$, b_n and $\mathcal{E} = \bigcup_{j\in\mathcal{J},s\in\mathcal{S}_j} e_{j,s}$, given by

$$r_{m,n,i}(\mathcal{A}_n, b_n, \mathcal{E}) = b_n w \log_2 \left(1 + \frac{p_m g_{m,i}}{\sum_{j\in\mathcal{J}} \sum_{s\in\mathcal{S}_j} a_{j,n} e_{j,s} p_{j,s} g_{j,i} + \sigma^2} \right) \tag{4}$$

where σ^2 is the average background noise power. The constraint of ED $i \in \mathcal{I}_n$ to successfully receive/decode the BL can be expressed as

$$r_{m,n,i}(\mathcal{A}_n, b_n, \mathcal{E}) \geq \lambda_{1,n}. \tag{5}$$

Let $\mathcal{I}_{j,n}$ be the set of EDs in $\mathcal{I}_n$ covered by UAV j. The ID of the ED in $\mathcal{I}_{j,n}$ with maximum channel gain is expressed as

$$i^*_{j,n} = \arg\max_{i\in\mathcal{I}_{j,n}} g_{j,i} \tag{6}$$

As the constraint of SIC and video layer reconstruction, the signal strength of the BL received by ED $i^*_{j,n}$ must be larger than that of the EL, and the decision variable, $e_{j,s}$, must satisfy

$$\sum_{s\in\mathcal{S}_j} e_{j,s} p_{j,s} g_{j,i^*_{j,n}} < \tau p_m g_{m,i^*_{j,n}} \tag{7}$$

where $\tau \in (0,1)$ is a parameter to adapt to the environment. It can also be expressed as

$$\sum_{s\in\mathcal{S}_j} e_{j,s} p_{j,s} - \tau p_m \frac{g_{m,i^*_{j,n}}}{g_{j,i^*_{j,n}}} \leq 0. \tag{8}$$

ED $i \in \mathcal{I}_{j,n}$ can receive the EL's signal. Because there is no NOMA layer superimposed on the EL, the signal of EL from UAV j with $p_{j,s}$ is not interfered with. The achievable rate of decoding the EL's signals at ED $i \in \mathcal{I}_{j,n}$ is expressed as a function of $\mathcal{A}_n$, b_n and $\mathcal{E}$, given by

$$r_{j,n,i}(\mathcal{A}_n, b_n, \mathcal{E}) = b_n w \log_2 \left(1 + \frac{\sum_{j\in\mathcal{J}} \sum_{s\in\mathcal{S}_j} a_{j,n} e_{j,s} p_{j,s} g_{j,i}}{\sigma^2} \right). \tag{9}$$

If both (5) and (10) are satisfied, the EL required by ED $i \in \mathcal{I}_{j,n}$ can be successfully received/decoded.

$$r_{j,n,i}(\mathcal{A}_n, b_n, \mathcal{E}) \geq \lambda_{2,n} \tag{10}$$

Take Fig. 4 as an example to illustrate the SIC decoding. The BL is propagated through signal $X_{1,n}$ with the BS's transmit power, and the EL is propagated through signal $X_{2,n}$ with the UAV's transmit power. $X_{1,n}$ and $X_{2,n}$ are sent simultaneously. EDs in $\mathcal{I}_{j,n}$ can decode $X_{1,n}$ and $X_{2,n}$ with the BL and EL. EDs in $\mathcal{I}_n \backslash \mathcal{I}_{j,n}$ can decode $X_{1,n}$ with the BL without SIC.

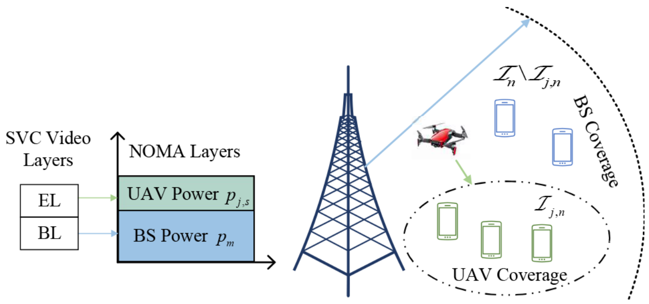

FIGURE 3 BS-UAV cooperative multicast in NOMA.

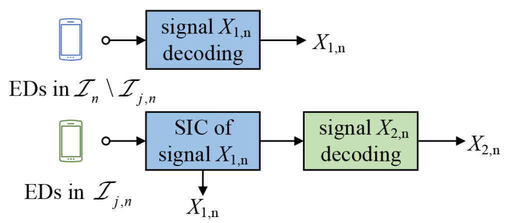

FIGURE 4 Interference cancellation in NOMA.

3 | PROBLEM FORMULATION

In the proposed UAV-assisted SVC video multicast framework, a challenging issue is to determine how to deploy UAVs, select transmit power and association patterns, and how many subchannels should be allocated to each multicast group.

Let $u_{1,n,i}$ be 1 if (5) is met, and be 0 otherwise. Let $u_{2,n,i}$ be 1 if both $u_{1,n,i} = 1$ and (10) are satisfied, and be 0 otherwise. The number of EDs who receive both the BL and EL in $\mathcal{I}_n$ is calculated by $\sum_{i\in\mathcal{I}_n} u_{2,n,i}$, and the number of EDs who only receive the BL in $\mathcal{I}_n$ is $\sum_{i\in\mathcal{I}_n} u_{1,n,i} - \sum_{i\in\mathcal{I}_n} u_{2,n,i}$. We use $\mathrm{PSNR}_{1,n}$ to denote the PSNR value of the BL received by multicast group n, and $\mathrm{PSNR}_{2,n}$ to represent the PSNR value when both the BL and EL can be obtained. The PSNR of video layers received by multicast group n with b_n subchannels is the summation of the two parts multiplied by $\mathrm{PSNR}_{2,n}$ and $\mathrm{PSNR}_{1,n}$, and can be expressed as a function of $\mathcal{V} = \bigcup_{j\in\mathcal{J}} v_j$, $\mathcal{A}_n$, b_n and $\mathcal{E}$, given by

$$f_n(\mathcal{V}, \mathcal{A}_n, b_n, \mathcal{E}) = \sum_{i\in\mathcal{I}_n} u_{2,n,i} \mathrm{PSNR}_{2,n} + \left(\sum_{i\in\mathcal{I}_n} u_{1,n,i} - \sum_{i\in\mathcal{I}_n} u_{2,n,i} \right) \mathrm{PSNR}_{1,n}. \tag{11}$$

The set of multicast groups along with its set cardinality are denoted as $\mathcal{N}$ and N. Based on (11), the aggregate PSNR for all multicast groups is expressed as a function of $\mathcal{V}$, $\mathcal{A} = \bigcup_{n\in\mathcal{N}} \mathcal{A}_n$, $\mathcal{B} = \bigcup_{n\in\mathcal{N}} b_n$, and $\mathcal{E}$, given by

$$f(\mathcal{V}, \mathcal{A}, \mathcal{B}, \mathcal{E}) = \sum_{n\in\mathcal{N}} f_n(\mathcal{V}, \mathcal{A}_n, b_n, \mathcal{E}). \tag{12}$$

The corresponding aggregate video receiving rate of all EDs is calculated as

$$\sum_{l\in\{1,2\}}\sum_{n\in\mathcal{N}}\sum_{i\in\mathcal{I}_n} u_{l,n,i}\lambda_{l,n}.$$

The joint optimization of UAV deployment, association patterns, spectrum partition and UAV transmit power control for maximizing (12) is formulated as

$$\mathcal{P}1:\max_{\mathcal{V},\mathcal{A},\mathcal{B},\mathcal{E}}:f(\mathcal{V},\mathcal{A},\mathcal{B},\mathcal{E})$$

$$\text{s.t.}\begin{cases} r_{m,n,i}(\mathcal{A}_n,b_n,\mathcal{E})-\varsigma u_{1,n,i}<\lambda_{1,n},\forall n,i & \text{(13a)}\\ r_{m,n,i}(\mathcal{A}_n,b_n,\mathcal{E})+\varsigma(1-u_{1,n,i})\geq\lambda_{1,n},\forall n,i & \text{(13b)}\\ r_{j,n,i}(\mathcal{A}_n,b_n,\mathcal{E})-\vartheta u_{2,n,i}u_{1,n,i}<\lambda_{2,n},\forall n,i & \text{(13c)}\\ r_{j,n,i}(\mathcal{A}_n,b_n,\mathcal{E})+\vartheta(1-u_{2,n,i})u_{1,n,i}\geq\lambda_{2,n},\forall n,i & \text{(13d)}\\ a_{j,n}\left(\sum_{s\in S_j}e_{j,s}p_{j,s}-\tau p_m\dfrac{g_{m,i^*_{j,n}}}{g_{j,i^*_{j,n}}}\right)\leq 0,\forall j,n & \text{(13e)}\\ \sum_{s\in S_j}e_{j,s}-1=0,\forall j & \text{(13f)}\\ \sqrt{x_j^2+y_j^2}\leq R_m,\forall j & \text{(13g)}\\ z^{(\min)}\leq z_j\leq z^{(\max)},\forall j & \text{(13h)}\\ \sum_{n\in\mathcal{N}}b_n\leq B & \text{(13i)}\\ \sum_{j\in\mathcal{J}}a_{j,n}\leq 1,\forall n & \text{(13j)}\\ e_{j,s}\in\{0,1\},\forall j,s & \text{(13k)}\\ u_{l,n,i}\in\{0,1\},\forall l\in\{1,2\},n,i & \text{(13l)}\\ a_{j,n}\in\{0,1\},\forall j,n & \text{(13m)} \end{cases}$$

In (13a) and (13b), ς is a large enough constant to guarantee

$$u_{1,n,i}=\begin{cases}1, r_{m,n,i}(\mathcal{A}_n,b_n,\mathcal{E})-\lambda_{1,n}>0\\ 0, r_{m,n,i}(\mathcal{A}_n,b_n,\mathcal{E})-\lambda_{1,n}\leq 0.\end{cases}\tag{14}$$

In (13c) and (13d), ϑ is a large enough constant to ensure

$$u_{2,n,i}=\begin{cases}1, (r_{j,n,i}(\mathcal{A}_n,b_n,\mathcal{E})-\lambda_{2,n})u_{1,n,i}>0\\ 0, (r_{j,n,i}(\mathcal{A}_n,b_n,\mathcal{E})-\lambda_{2,n})u_{1,n,i}\leq 0.\end{cases}\tag{15}$$

Constraint (13e) is derived from (8). Constraint (13f) ensures that each UAV can only select one transmit power. Constraint (13g) states that each UAV's x-y axis position must be within the BS coverage, where R_m represents the BS's coverage radius. Constraint (13h) is the flying height scope, [$z^{(\min)}$, $z^{(\max)}$], as in Fig. 2, of each UAV. Constraint (13i) prevents the resource allocation for all multicast groups from exceeding the total number of subchannels. Under (13j), each multicast group can only associate with one UAV.

It is noted that ($\mathcal{P}1$) contains integer variables $e_{j,s}, b_n, a_{j,n}$ and continuous variable(s) $v_j(x_j,y_j,z_j)$. The non-linear combinatorial transformation of the integer variables and the transformation of the continuous variables is conditioned by the objective and constraints. Thus, ($\mathcal{P}1$) belongs to a class of MINLP problem, which is generally NP-hard, and designing efficient algorithms to get a suboptimal solution is necessary.

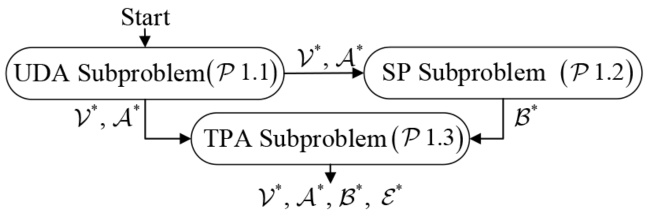

FIGURE 5 Problem-solving framework.

4 | SOLUTIONS

($\mathcal{P}1$) is decomposed to the UDA, SP, and TPA subproblems to make it tractable and handleable. Problem-solving consists of three sequential steps, as illustrated in Fig. 5: 1) The UAV deployment positions , $\mathcal{V}^*$, and the association patterns, $\mathcal{A}^*$, are obtained by the UDA subproblem; 2) Given $\mathcal{V}^*$ and $\mathcal{A}^*$, the SP subproblem is solved to obtain the spectrum partition scheme, $\mathcal{B}^*$; 3) Based on $\mathcal{A}^*$, $\mathcal{V}^*$ and $\mathcal{B}^*$, the optimal UAV transmit power scheme, $\mathcal{E}^*$, is obtained by solving the TPA subproblem. We next discuss the implementation details.

4.1 | Solution to the UDA Subproblem

According to the UAV coverage model in Section 2.2, the number of EDs served by UAVs depends mainly on the flight height, given UAV deployment positions on the x-y plane. Therefore, we first determine the positions against hotspot areas on the x-y plane via k-means [28] and then adjust UAVs' height.

The UDA subproblem aims to maximize the number of EDs under UAVs' coverage while optimizing transmission performance through UAV flight height adjustment. Under the condition that the number of EDs served by UAV j (i.e., $\sum_{n\in\mathcal{N}} I_{j,n}$) remains unchanged, UAV j should reduce flying height z_j to improve transmission quality. For this purpose, the UAV flight altitude is determined as

$$z_j^*=\arg\min_{z_j\in[z^{(\min)},z^{(\max)}]}\left(\sum_{n\in\mathcal{N}}I_{j,n}+\frac{R_j}{\alpha}\right),\forall j\in\mathcal{J}\tag{16}$$

where α is a constant to ensure $\frac{R_j}{\alpha}\in(0,1)$. Combining (16), the UDA subproblem is formulated as ($\mathcal{P}1.1$).

$$\mathcal{P}1.1:\max_{\mathcal{V},\mathcal{A}}\sum_{j\in\mathcal{J}}\sum_{n\in\mathcal{N}}a_{j,n}I_{j,n}$$

$$\text{s.t. (13g) (13h) (13j) (16).}\tag{17}$$

The locations of all EDs and the number of UAVs are fed into k-means for clustering. The centroids in the output correspond to UAVs' deployment positions on the x-y plane, denoted by $\bigcup_{j\in\mathcal{J}}(x_j^*, y_j^*)$. Combining (x_j^*, y_j^*) with z_j^* in (16), UAV j is located at $v_j^* = (x_j^*, y_j^*, z_j^*)$, and the set of UAV deployment positions, $\mathcal{V}^* = \bigcup_{j\in\mathcal{J}} v_j^*$, is obtained. The ID of the UAV associated with multicast group n is expressed as

$$j_n^* = \arg\max_{j\in\mathcal{J}} I_{j,n}. \tag{18}$$

Based on (18), the association pattern between multicast group n and UAV j is determined as

$$a_{j,n}^* = \begin{cases} 1, \text{if } j = j_n^* \\ 0, \text{otherwise} \end{cases} \tag{19}$$

which maximizes the number of EDs in the group (i.e., $\mathcal{I}_n$) under the coverage of UAV j. and the set of the association scheme, $\mathcal{A}^* = \bigcup_{n\in\mathcal{N}, j\in\mathcal{J}} a_{j,n}^*$, is obtained.

4.2 | Solution to the SP Subproblem

The spectrum partition relies on UAV transmit power. Note that a UAV may be associated with multiple multicast groups. For each multicast group that associates with UAV j, the transmit power of the UAV needs to satisfy (13e). Thus, the transmit power of UAV j is initialized as

$$\hat{s}_j = \arg\min_{n\in\mathcal{N}} \left(\max_{s\in\mathcal{S}_j} a_{j,n} \left(p_{j,s} - \tau p_m \frac{g_{m,i_{j,n}^*}}{g_{j,i_{j,n}^*}} \right) \right). \tag{20}$$

The corresponding decision variable is determined by

$$\hat{e}_{j,s} = \begin{cases} 1, \text{if } s = \hat{s}_j \\ 0, \text{otherwise.} \end{cases} \tag{21}$$

By substituting $\mathcal{V}^*$, $\mathcal{A}^*$ and $\hat{\mathcal{E}} = \bigcup_{j\in\mathcal{J}, s\in\mathcal{S}} \hat{e}_{j,s}$ into ($\mathcal{P}1$), ($\mathcal{P}1$) is reformulated as ($\mathcal{P}1.2$) with reduced variables.

$$\mathcal{P}1.2 : \max_{\mathcal{B}} : f(\mathcal{V}^*, \mathcal{A}^*, \mathcal{B}, \hat{\mathcal{E}})$$

$$\text{s.t. (13a) (13b) (13c) (13d) (13i) (13l).} \tag{22}$$

We now derive the upper bound of the number of subchannels allocated to multicast group n. Based on (4), (9), (18), and (21), in the case of $b_n = 1$, the minimum receiving rates for BL and EL at ED $i \in \mathcal{I}_n$ are calculated as

$$k_{1,n} = w \min_{i\in\mathcal{I}_n} \log_2 \left(1 + \frac{p_m g_{m,i}}{\sum_{j\in\mathcal{J}} \sum_{s\in\mathcal{S}_j} a_{j,n}^* \hat{e}_{j,s} p_{j,s} g_{j,i} + \sigma^2} \right) \tag{23}$$

and

$$k_{2,n} = w \min_{i\in\mathcal{I}_{j,n}} \log_2 \left(1 + \frac{\sum_{j\in\mathcal{J}} \sum_{s\in\mathcal{S}_j} a_{j,n}^* \hat{e}_{j,s} p_{j,s} g_{j,i}}{\sigma^2} \right). \tag{24}$$

According to (23) and (24), the upper bound of the number of subchannels allocated to multicast group n for a video layer is approximated as

$$b_n^{(\max)} = \max \left\{ \left\lceil \frac{\lambda_{1,n}}{k_{1,n}} \right\rceil, \left\lceil \frac{\lambda_{2,n}}{k_{2,n}} \right\rceil \right\}. \tag{25}$$

For the remaining b subchannels, the maximum PSNR of the first n multicast groups is marked as $F(n, b)$. If $b \geq b_n^{(\max)}$, we only consider allocating $[0, b_n^{(\max)}]$ subchannels to multicast group n.

Based on a recursion for (26), Algorithm 1 is designed to find the optimal solution for spectrum partition. The algorithm belongs to an upgraded knapsack via dynamic programming. N multicast groups can be regarded as N types of items, and each type has B items. These items need to be put in a knapsack with a capacity of B. The b_nth item in the nth class has a profit (determined by $f_n(\mathcal{V}^*, \mathcal{A}_n^*, b_n, \hat{\mathcal{E}})$) and a weight (i.e., b_n). The essence is to select one item from each type to maximize the total profit while the total weight does not exceed the capacity. $F(n, b)$ is computed recursively from $n = 1$ and $b = 1$, which relies on the maximum total PSNR of the first $n - 1$ multicast group(s) and $f_n(\mathcal{V}^*, \mathcal{A}_n^*, b_n, \hat{\mathcal{E}})$. Based on (26), inappropriate subchannel numbers are filtered to reduce unnecessary calculations. After NB iterations, the optimal total PSNR (i.e., $F(N, B)$) and the spectrum allocation scheme (i.e., $\mathcal{B}^* = \bigcup_{n\in\mathcal{N}} b_n^*$) can be obtained.

Algorithm 1 Spectrum Partition

Input: $\mathcal{V}^*, \mathcal{A}^*, B, \hat{\mathcal{E}}$
Output: $\mathcal{B}^*$

```
m ← 0;
for b ← 1 to B do
    F(0, b) ← 0;
end for
for n ← 1 to N do
    for b ← 1 to B do
        b*_n ← 0;
        F(n, b) ← F(n − 1, b);
        for b' ← 1 to b do
            if b' > b_n^(max) then
                break;
            end if
            m ← F(n − 1, b − b') + f_n(V*, A*_n, b', Ê);
            if F(n, b) < m then
                F(n, b) ← m; b*_n ← b';
            end if
        end for
    end for
end for
return B* = ⋃_{n∈N} b*_n;
```

$$F(n,b) = \begin{cases} \max_{0 \le b_n \le b} F(n-1, b-b_n) + f_n(\mathcal{V}^*, \mathcal{A}_n^*, b_n, \widehat{\mathcal{E}}), \text{if } b < b_n^{(\max)} \\ \max_{0 \le b_n \le b_n^{(\max)}} F(n-1, b-b_n) + f_n(\mathcal{V}^*, \mathcal{A}_n^*, b_n, \widehat{\mathcal{E}}), \text{if } b \ge b_n^{(\max)} \end{cases} \tag{26}$$

4.3 | Solution to the TPA Subproblem

Since the resource utilization is confined to the initialized UAV transmit power determined by (21), it is necessary to perform power fine-tuning to boost performance. Given $\mathcal{V}^*$, $\mathcal{A}^*$ and $\mathcal{B}^*$, the TPA subproblem is formulated as

$$\mathcal{P}1.3 : \max_{\mathcal{E}} : f(\mathcal{V}^* \mathcal{A}^*, \mathcal{B}^*, \mathcal{E})$$

$$\text{s.t. (13a) (13b) (13c) (13d) (13e) (13f) (13k) (13l).} \tag{27}$$

Since there is no coupling among decision variables in $\mathcal{E}$, ($\mathcal{P}1.3$) can be transformed as maximizing the aggregate PSNR of the multicast groups associated with UAV j, expressed as

$$\sum_{n \in \mathcal{N}} a_{j,n}^* f_n(\mathcal{V}^*, \mathcal{A}_n^*, b_n^*, \mathcal{E}).$$

A fast search policy is developed in Algorithm 2 to optimize the transmit power of each UAV. Assume that all indexes are sorted in an ascending order of UAV transmit power. The algorithm searches downwards starting from the initialized power (line 3), $\widehat{s}_j$, to speed up the search. In other words, the strategic space of transmit power for UAV j is reduced to

$$\widehat{S}_j = \{s \in S_j | p_{j,s} \le p_{j,\widehat{s}_j}\}. \tag{28}$$

Algorithm 2 Fast Transmit Power Fine-Tuning

Input: $\mathcal{V}^*, \mathcal{A}^*, \mathcal{B}^*, \widehat{s}_j$
Output: $\mathcal{E}^*$

1: **for** $j' \leftarrow 1$ to J **do**
2: $\quad t' \leftarrow 0; t \leftarrow 0;$
3: $\quad$ **for** $s' \leftarrow \widehat{s}_j$ to 1 **do**
4: $\quad\quad$ Every element in $\mathcal{E}$ is set to 0;
5: $\quad\quad e_{j',s'} \leftarrow 1;$
6: $\quad\quad t \leftarrow \sum_{n \in \mathcal{N}} a_{j,n}^* f_n(\mathcal{V}^*, \mathcal{A}_n^*, b_n^*, \mathcal{E});$
7: $\quad\quad$ **if** $t > t'$ **then**
8: $\quad\quad\quad t' \leftarrow t; \mathcal{E}^* \leftarrow \mathcal{E};$
9: $\quad\quad$ **end if**
10: $\quad$ **end for**
11: **end for**
12: **return** $\mathcal{E}^*$;

TABLE 2 Parameter settings

Parameters	Values
Altitude of the BS (z_m)	10 m
Coverage radius of the BS (R_m)	800 m
BS transmit power (p_m)	10000 mW
Optional UAV transmit power ($p_{j,s}$)	{1,2,...,8} mW
Scope of UAV flying height ($[z^{(\min)}, z^{(\max)}]$)	[10 m,190 m]
Parameters of UAV ($o_1/o_2/\eta_{\text{LoS}}/\eta_{\text{NLoS}}$)	9.61/0.16/1/20
Carrier frequency (c_1)	3.5 GHz [30]
LoS probability threshold (ξ)	0.5
Free space path-loss threshold (ψ)	89 dB
Average background noise power (σ^2)	-174 dBm
Power parameter (τ)	0.8
Subchannel bandwidth (w)	180 kHz
Number of subchannels (B)	8-16
Number of multicast groups (N)	7
Number of EDs for multicast group n (I_n)	35

4.4 | Computational Complexity Analysis

In ($\mathcal{P}1.1$), the complexity of k-means is $O\left(\sum_{n \in \mathcal{N}} I_n\right)$, and association pattern calculations need to search for all $1 \le n \le N$ and $1 \le j \le J$, with a complexity of $O(NJ)$. For ($\mathcal{P}1.2$), the PSNR for multicast group n with b_n subchannels (determined by $f_n(\mathcal{V}^*, \mathcal{A}_n^*, b_n, \widehat{\mathcal{E}})$) should be computed over all $1 \le n \le N$ and $1 \le b \le B$, and every iteration has a maximum complexity of $O(B)$. Thus, the worst-case complexity is $O(NB^2)$. Based on (28), the complexity of Algorithm 2 for solving ($\mathcal{P}1.3$) is $O(\sum_{j \in \mathcal{J}} \widehat{S}_j)$, where $\widehat{S}_j$ is the cardinality of $\widehat{S}_j$. The accumulative computational complexity reaches $O(\sum_{n \in \mathcal{N}} I_n + NJ + NB^2 + \sum_{j \in \mathcal{J}} \widehat{S}_j)$, which is lower than complexity of ($\mathcal{P}1$). We later verify whether the proposed scheme can approach the optimal solution or directly hit it.

5 | PERFORMANCE EVALUATION

5.1 | Experiment Design

Extensive numerical simulations are conducted to verify the effectiveness and superiority of the proposed solution through MATLAB. Real video trace from [29], consisting of ten standard video test sequences with different video layers, along with the average bite rate and the PSNR of each video layer, is utilized to make simulations more realistic. The detailed parameter setting is listed in Table 2.

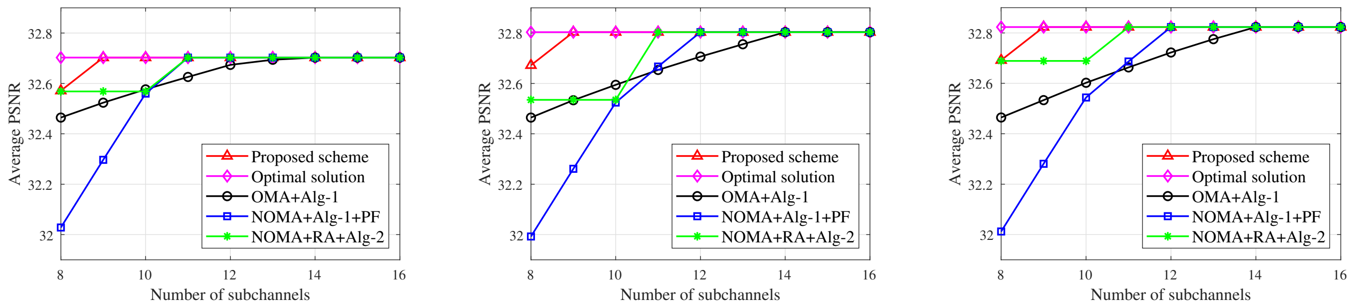

(a) 2 UAVs (b) 3 UAVs (c) 4 UAVs

FIGURE 6 Average PSNR for each ED with varing subchannels

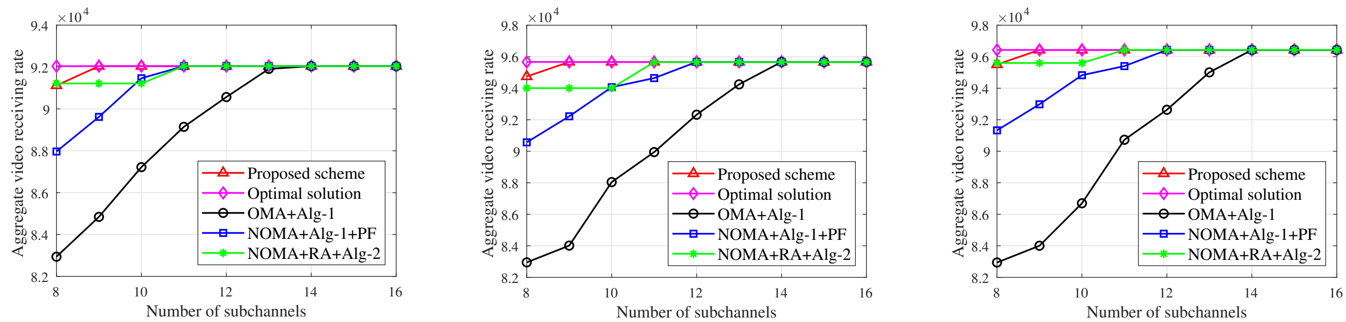

(a) 2 UAVs (b) 3 UAVs (c) 4 UAVs

FIGURE 7 Aggregate video receiving rate with varing subchannels

To evaluate the performance of the proposed strategy, we compare it with the optimal solution and the other four baseline schemes which are introduced in the following.

- **Optimal Solution**, which relies on exhaustion to find the optimal solution to observe how the proposed method approaches the upper bound on performance.
- **OMA+Alg-1** [2], in which the BS and UAV multicast the BL and EL to a multicast group over orthogonal channels with fixed transmit power.
- **NOMA+Alg-1+Power Fixed (PF)** [21], which focuses on optimizing spectrum resource allocation without considering UAV transmit power.
- **NOMA+Resource Averaging (RA)+Alg-2**, which adjusts UAV transmit power via Algorithm 2 and equally allocate subchannels among N multicast group.

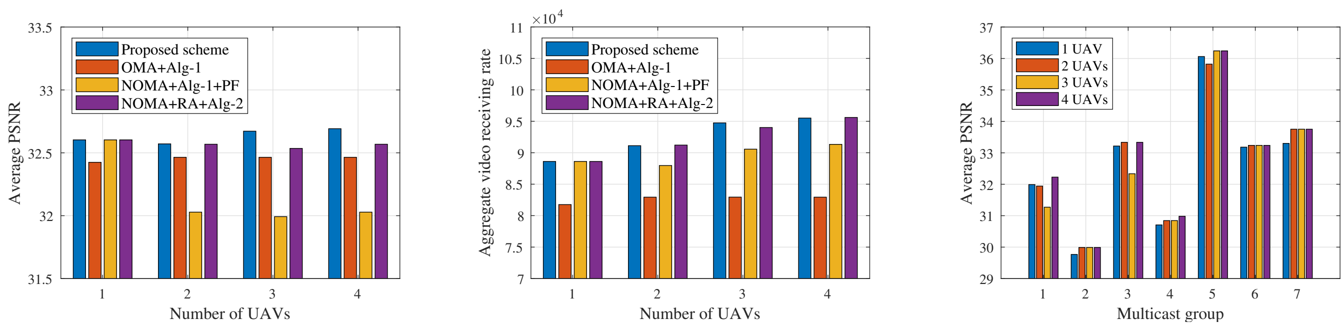

(a) Average PSNR for each ED (b) Aggregate video receiving rate (c) Average PSNR for each multicast group

FIGURE 8 Average PSNR and aggregate video receiving rate with varying number of UAVs

5.2 | Result Analysis

Impact of the number of available subchannels: Fig. 6 shows the average PSNR for each ED as the number of subchannels varies from 8 to 16. Three subfigures are generated further to observe the effect of the number of UAVs. With the increase of b_n that can support the transmission of more video layers, the average PSNR for each scheme shows a growing tendency and tends to be unchanged when B is large enough. First, the proposed plan consumes lower spectrum resources than the OMA-based solution. Second, the proposed scheme can achieve more average PSNR than OMA+Alg-1, even with few spectrum resources. Since the proposed UAV transmit power adaptation scheme mitigates EL signals' interference with BL signals, our proposed method improves by 0.5dB over the NOMA+Alg-1+PF, when $J = 4$ and $B = 8$. Third, the proposed spectrum partition outperforms the resource averaging strategy of NOMA+RA+Alg-2. Fig. 7 shows the aggregate video receiving rate with the same parameters as Fig. 6. Compared with the OMA+Alg-1, our scheme's aggregate video receiving rate has increased by 15% when $J = 4$ and $B = 8$. We can see that the proposed scheme achieves the highest PSNR and aggregate video receiving rate, approximating or directly obtaining the optimal solution.

Impact of the number of UAVs: Fig. 8 depicts the average PSNR and aggregate video receiving rate as the number of UAVs varies from 1 to 4 with B fixed to 8. The increase in the number of UAVs enables more EDs to be covered, which boosts the average PSNR and aggregate video receiving rate. In OMA+Alg-1, the resources used to transmit the BL are insufficient. Even with more available UAVs, the increase in average PSNR is hard-to-achieve. The closer the EDs' hotspot is to the edge of the BS coverage, the worse the channel conditions. In NOMA+Alg-1+PF, UAVs' transmit power fails to adapt to heterogeneous channel conditions. Thanks to the efficient resource utilization in NOMA and the transmit power adaptation, the proposed scheme is superior to the other three schemes. Especially when resources are scarce, the video service in hotspot areas can be prioritized to boost overall performance. Differences in the number of UAVs lead to different UAV placement via k-means clustering and association patterns. From Fig. 8(c), an increase in the number of UAVs improves the received video quality in most cases.

6 | CONCLUSION

We have presented NOMA enhanced SVC multicast scheme in UAV-assisted RANs. Resource management is studied to maximize the aggregate PSNR received by all the EDs. Since this joint optimization problem of UAV deployment, association patterns between UAVs and multicast groups, spectrum allocation, and UAV transmit power selection is an MINLP problem, it is decoupled into three subproblems to facilitate this solution. Low-complexity heuristic algorithms are devised to determine UAV deployment, association patterns, spectrum allocation, and UAV transmit power. Simulation results with real-trace confirm that the proposed scheme improves significantly over other benchmarks. Our ongoing work plans to develop a dynamic UAV cooperative deployment mechanism to adapt to complex video service scenarios.

References

1. Ioan-Sorin Comşa, Gabriel-Miro Muntean, and Ramona Trestian, *An innovative machine-learning-based scheduling solution for improving live UHD video streaming quality in highly dynamic network environments*, IEEE Trans. Broadcast. **67** (2021), no. 1, 212–224.
2. Hao Zhu, Yang Cao, Tao Jiang, and Qian Zhang, *Scalable NOMA multicast for SVC streams in cellular networks*, IEEE Trans. Commun. **66** (2018), no. 12, 6339–6352.
3. Mojtaba Ghermezcheshmeh, Vahid Shah-Mansouri, and Mohammad Ghanbari, *Analysis and performance evaluation of scalable video coding over heterogeneous cellular networks*, Computer Networks **148** (2019), 151–163.
4. Linglong Dai, Bichai Wang, Yifei Yuan, Shuangfeng Han, I. Chih-lin, and Zhaocheng Wang, *Non-orthogonal multiple access for 5G: Solutions, challenges, opportunities, and future research trends*, IEEE Commun. Mag. **53** (2015), no. 9, 74–81.
5. Zhiguo Ding, Yuanwei Liu, Jinho Choi, Qi Sun, Maged Elkashlan, I. Chih-Lin, and H. Vincent Poor, *Application of non-orthogonal multiple access in LTE and 5G networks*, IEEE Commun. Mag. **55** (2017), no. 2, 185–191.
6. Ming Zhang, Hancheng Lu, Feng Wu, and Chang Wen Chen, *NOMA-based scalable video multicast in mobile networks with statistical channels*, IEEE Trans. Mobile Comput. **20** (2021), no. 6, 2238–2253.
7. Hang Shen, Qiang Ye, Weihua Zhuang, Weisen Shi, Guangwei Bai, and Geng Yang, *Drone-small-cell-assisted resource slicing for 5G uplink radio access networks*, IEEE Trans. Veh. Technol. **70** (2021), no. 7, 7071–7086.
8. Nan Zhao, F. Richard Yu, Lisheng Fan, Yunfei Chen, Jie Tang, Arumugam Nallanathan, and Victor C.M. Leung, *Caching unmanned aerial vehicle-enabled small-cell networks: Employing energy-efficient methods that store and retrieve popular content*, IEEE Veh. Technol. Mag. **14** (2019), no. 1, 71–79.
9. S. M. Riazul Islam, Nurilla Avazov, Octavia A. Dobre, and Kyung-sup Kwak, *Power-domain non-orthogonal multiple access (NOMA) in 5G systems: Potentials and challenges*, IEEE Commun. Surveys Tuts. **19** (2017), no. 2, 721–742.
10. Aziz Altaf Khuwaja, Yunfei Chen, Nan Zhao, Mohamed-Slim Alouini, and Paul Dobbins, *A survey of channel modeling for UAV communications*, IEEE Commun. Surveys Tuts. **20** (2018), no. 4, 2804–2821.
11. Yuan Wu, Li Ping Qian, Haowei Mao, Xiaowei Yang, HaiBo Zhou, and Xuemin Shen, *Optimal power allocation and scheduling for non-orthogonal multiple access relay-assisted networks*, IEEE

Trans. Mobile Comput. **17** (2018), no. 11, 2591–2606.
12. Gang Liu, Zhiqing Wang, Jiewen Hu, Zhiguo Ding, and Pingzhi Fan, *Cooperative NOMA broadcasting/multicasting for low-latency and high-reliability 5G cellular V2X communications*, IEEE Internet Things J. **6** (2019), no. 5, 7828–7838.
13. Sungjun Ahn, Sung-Ik Park, Jae-Young Lee, Namho Hur, and Joonhyuk Kang, *Cooperation between ldm-based terrestrial broadcast and broadband unicast: On scalable video streaming applications*, IEEE Trans. Broadcast. **67** (2021), no. 1, 2–22.
14. Hao Zhou, Yusheng Ji, Xiaoyan Wang, and Baohua Zhao, *Joint resource allocation and user association for SVC multicast over heterogeneous cellular networks*, IEEE Trans. Wireless Commun. **14** (2015), no. 7, 3673–3684.
15. Giuseppe Araniti, Federica Rinaldi, Pasquale Scopelliti, Antonella Molinaro, and Antonio Iera, *A dynamic MBSFN area formation algorithm for multicast service delivery in 5G NR networks*, IEEE Trans. Wireless Commun. **19** (2020), no. 2, 808–821.
16. Xiaoda Jiang, Hancheng Lu, and Chang Wen Chen, *Enabling quality-driven scalable video transmission over multi-user NOMA system*, IEEE INFOCOM, 2018, pp. 1952–1960.
17. Sungjun Ahn, Sung-Ik Park, Jae-Young Lee, Namho Hur, Yiyan Wu, Liang Zhang, Wei Li, and Jeongchang Kim, *Large-scale network analysis on noma-aided broadcast/unicast joint transmission scenarios considering content popularity*, IEEE Trans. Broadcast. **66** (2020), no. 4, 770–785.
18. Xiaowei Pang, Zan Li, Xiaoming Chen, Yang Cao, Nan Zhao, Yunfei Chen, and Zhiguo Ding, *UAV-aided NOMA networks with optimization of trajectory and precoding*, International Conference on Wireless Communications and Signal Processing (WCSP), 2018, pp. 1–6.
19. Pang X, J. Tang, N. Zhao, Zhang X, and Qian Y, *Energy-efficient design for mmwave-enabled noma-uav networks*, Sci. China Inf. Sci. **64** (2021), no. 4, 14.
20. Minh Dat Nguyen, Long Bao Le, and Andr Girard, *Trajectory control and resource allocation for UAV-based networks with wireless backhauls*, IEEE ICC, 2021, pp. 1–6.
21. Daosen Zhai, Huan Li, Xiao Tang, Ruonan Zhang, Zhiguo Ding, and Fei Richard Yu, *Height optimization and resource allocation for NOMA enhanced UAV-aided relay networks*, IEEE Trans. Commun. **69** (2021), no. 2, 962–975.
22. Amin Farajzadeh, Ozgur Ercetin, and Halim Yanikomeroglu, *UAV data collection over noma backscatter networks: UAV altitude and trajectory optimization*, IEEE ICC, 2019, pp. 1–7.
23. Wei Wang, Jie Tang, Nan Zhao, Xin Liu, Xiu Yin Zhang, Yunfei Chen, and Yi Qian, *Joint precoding optimization for secure SWIPT in UAV-aided NOMA networks*, IEEE Trans. Commun. **68** (2020), no. 8, 5028–5040.
24. M. S. Shokry, D. Ebrahimi, C. Assi, S. Sharafeddine, and A. Ghrayeb, *Leveraging UAVs for coverage in cell-free vehicular networks: A deep reinforcement learning approach*, IEEE Trans. Mobile Comput. **20** (2021), no. 9, 2835 – 2847.
25. Xiaoyan Hu, Kai-Kit Wong, and Yangyang Zhang, *Wireless-powered edge computing with cooperative uav: Task, time scheduling and trajectory design*, IEEE Trans. Wireless Commu. **19** (2020), no. 12, 8083–8098.
26. Akram Al-Hourani, Sithamparanathan Kandeepan, and Simon Lardner, *Optimal LAP altitude for maximum coverage*, IEEE Wireless Commun. Lett. **3** (2014), no. 6, 569–572.
27. Weisen Shi, Junling Li, Wenchao Xu, Haibo Zhou, Ning Zhang, Shan Zhang, and Xuemin Shen, *Multiple drone-cell deployment analyses and optimization in drone assisted radio access networks*, IEEE Access **6** (2018), 12518–12529.
28. Hua Qu, Wenna Zhang, Jihong Zhao, Zhirong Luan, and Chen Chang, *Rapid deployment of UAVs based on bandwidth resources in emergency scenarios*, Information Communication Technologies Conference (ICTC), 2020, pp. 86–90.
29. Joohyung Lee, Byung Chul Yeo, Ji-Su Kim, Min Seok Jang, and Jun Kyun Choi, *Energy efficient scalable video coding based cooperative multicast scheme with selective layer forwarding*, IEEE Wireless Commun. Lett. **17** (2013), no. 6, 1116–1119.
30. Ioannis-Prodromos Belikaidis, Andreas Georgakopoulos, Evangelos Kosmatos, Valerio Frascolla, and Panagiotis Demestichas, *Management of 3.5-GHz spectrum in 5G dense networks: A hierarchical radio resource management scheme*, IEEE Veh. Technol. Mag. **13** (2018), no. 2, 57–64.

AUTHOR BIOGRAPHY

Ziyuan Tong received the B.S. degree in Computer Science from the Nanjing University Jinling College, Nanjing, China. She is currently an M.S. student at the Department of Computer Science and Technology, Nanjing Tech University, Nanjing, China. Her research interests include space-air-ground integrated networks, non-orthogonal multiple access, resource management, and layer-aware wireless multicasting.

Hang Shen is currently an Associate Professor with the Department of Computer Science and Technology, Nanjing Tech University, Nanjing, China. He received the Ph.D. degree (with honors) in Computer Science from the Nanjing University of Science and Technology. He worked as a Full-Time Postdoctoral Fellow with the Broadband Communications Research (BBCR) Lab, Department of Electrical and Computer Engineering, University of Waterloo, Waterloo, ON, Canada, from 2018 to 2019. His research interests involve space-air-ground integrated networks, network security and privacy computing. He serves as an Associate Editor for the IEEE ACCESS, an Academic Editor for the *Mathematical Problems in Engineering*, and served as a Guest Editor for the *Peer-to-Peer Networking and Applications*.

Shi Ning holds a bachelor's degree from Tsinghua University and a doctorate from Hong Kong University of Science and Technology. He is a leading domestic researcher in supply chain management and blockchain research. He is also a young and middle-aged leading talent in the field of cybersecurity and informatization of the Internet Information Office of the Jiangsu Provincial Party Committee, a talented person in innovation and innovation of Jiangsu Province, and a top expert in Nanjing. He used to be a senior researcher at IBM China Research Institute and a professor at the School of Management of Sun Yat-sen University. He is currently the dean of Nanjing Trusted Blockchain and Algorithm Economics Institute, the chairman of Nanjing Jinninghui Technology, the visiting professor of Macau University of Science and Technology, the consultant of the Strategy Committee of Nanjing Digital Finance Industry Research Institute, and the chief scientist of the "Blockchain Industry Finance" laboratory of Foshan Rural Commercial Bank. He has presided over or participated in more than 10 National Natural Science Foundation projects, and published more than 30 high-quality papers. He has 57 invention patents in the blockchain field, and obtained 53 software copyrights. He has served as a member of several academic committees. He was named a highly cited scholar in China's decision science field by Elsevier for six consecutive years, and one of the most influential scholars in China's decision science field.

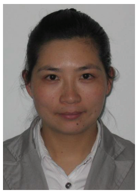

Tianjing Wang holds a BSc. (2000) in Mathematics at the Nanjing Normal University, a MSc. (2005) in Mathematics at the Nanjing University, and a Ph.D. (2009) in Signal and Information System at the Nanjing University of Posts and Telecommunications. From 2011 to 2013, she was a postdoctoral fellow with the School of Electronic Science and Engineering, Nanjing University of Posts and Telecommunications. From 2013 to 2014, she was a visiting scholar with the Department of Electrical and Computer Engineering, State University of New York at Stony Brook. She is now an Associate Professor in Mathematics at the Nanjing Tech University. Her research interests include vehicular networks, UAV networking and communications.

Guangwei Bai received the B.Eng. and M.Eng. degrees in computer engineering from Xi'an Jiaotong University, Xi'an, China, in 1983 and 1986, respectively, and the Ph.D. degree in Computer Science from the University of Hamburg, Hamburg, Germany, in 1999. From 1999 to 2001, he worked at the German National Research Center for Information Technology, Germany, as a Research Scientist. In 2001, he joined the University of Calgary, Calgary, AB, Canada, as a Research Associate. Since 2005, he has been working at Nanjing Tech University, Nanjing, China, as a Professor in Computer Science. From October to December 2010, he was a Visiting Professor with the Department of Electrical and Computer Engineering, University of Waterloo, Waterloo, ON, Canada. His research interests include architecture and protocols design for communication networks, multimedia networking, network security, and location-based services. He is a member of the ACM and a Distinguished Member of CCF.